Solid-State Reactions

DOI: 10.1002/ange.201103386

Solid-State Redox Solutions: Microfabrication and Electrochemistry**

Dezhi Yang, Lianhuan Han, Yang Yang, Liu-Bin Zhao, Cheng Zong, Yi-Fan Huang, Dongping Zhan, and Zhong-Qun Tian*

The miniaturization and integration of functional components is of significance in microelectromechanical systems (MEMS), ultralarge-scale integration circuit (ULSI), and miniaturized total analysis systems (μ-TAS).[1,2] Electrochemical methods are widely used in not only synthesizing functional materials, but also constructing these functional materials into microdevices, such as microsensors, microactuators, motors, and electrocolorimeters.[3,4] For example, a few redox couples were constructed into a microfluidic chip as an electrochemical logic device.[5] Note that the presence of liquid electrolyte is crucial and impractical in these microdevices, especially when their sizes are decreased to micro- or nanometer scale. Alternatively, it is possible to construct a solid-state electrochemical device. Solid-state electrochemistry has been studied for decades.[6,7] To our knowledge, however, it has not been used yet in microfabrication.

It is well-known that $Na_4Fe(CN)_6$ and $Na_3Fe(CN)_6$ can replace the NaCl lattice units to form the so called "solid-state solution".[11–14] Owing to its specific electronic and vibrational properties, it has wide application as photographic and scintillators materials. In general, such solid-state solutions were obtained at ambient temperature by slow evaporation of saturated aqueous solution of NaCl containing ion hexacyanides. Herein we present a novel technique for surface microfabrication of submicrometer-sized solid-state electrolyte of NaCl crystals containing redox couples, which would promote practical application of solid-state electrochemical system in microdevices.

Our technique is based on a scanning microcapillary-supported electrochemical microcell (Figure 1 a).[8,9] The microcapillary has a submicrometer- or micrometer-sized orifice, which forms a microcell with a large substrate of either ITO or Au thin film coated on glass cover slide. An Ag/AgCl wire inserted into the micropipette serves as both reference and counter electrodes. Owing to the capillary force, the liquid electrolyte at the opening of the microcapillary contacts the substrate surface with a limited tiny amount of volume so

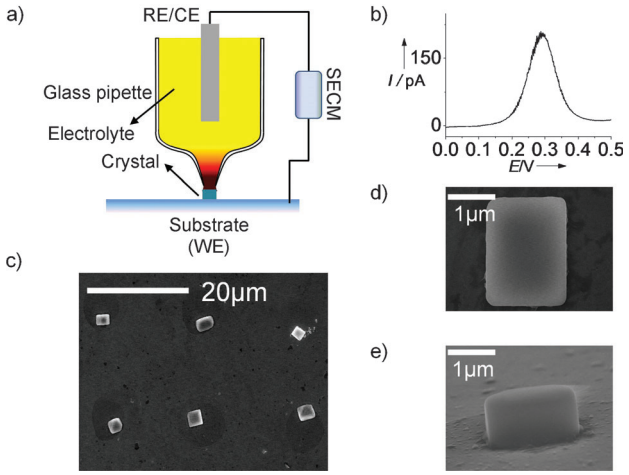

Figure 1. a) The scanning microcapillary-based electrochemical microsystem, where SECM is a scanning electrochemical microscopy workstation used for electrochemical modulation and also 3D control of the microcapillary. b) The linear scanning voltammogram recorded during the microfabrication of the microcrystals; the aqueous solution inside the microcapillary contains 1.0×10^{-5} mol L^{-1} $Na_4Fe(CN)_6$ and 0.05 mol L^{-1} NaCl, scanning rate is 0.1 V s^{-1}. c) SEM images of the microcrystal array. d) Top view of a typical microcrystal, and e) side view of the microcrystal in (d).

that electrochemical reactions are confined within the limited contact region. When the electrochemical microsystem is set up, linear voltammetry is performed (Figure 1 b). Consequently, a cubic microcrystal is formed. The scanning microcapillary is moved to the next spot until a microcrystal array is fabricated. Figure 1 d,e demonstrate the top and side views of a typical microcrystal from Figure 1 c.

As the electrolyte has a pico- or femtoliter volume exposed to air, the evaporation of water should be avoided strictly in the scanning microcapillary experiments.[8,9] Distinct from all the previously reported work, the well-shaped single microcrystals were obtained by benefiting from the evaporation of water in the ambient environment. From the data in Figure 1 b, the theoretically estimated concentration of $Fe(CN)_6^{4-}$ is 20 more times higher in the vicinity of substrate surface than in the bulk. The symmetric current peak shows the characteristic of thin-layer electrolysis, indicating that $Fe(CN)_6^{3-/4-}$ couples are trapped in the concentrated electrolyte drop between the substrate and the microcapillary. Water evaporation makes the supersaturated precondition for microcrystal formation. Second, the percentage of iron hexacyanide in the solid state solution is adjustable through changing the concentration of $Na_4Fe(CN)_6$ in the NaCl solution.[10–13] As shown in the Supporting Information, S1, the Raman intensity of the single mirocrystal

[*] D. Yang, L. Han, Y. Yang, L.-B. Zhao, C. Zong, Y.-F. Huang, Prof. Dr. D. Zhan, Prof. Dr. Z.-Q. Tian
Department of Chemistry, College of Chemistry and Chemical Engineering, and State Key Laboratory of Physical Chemistry of Solid Surfaces, Xiamen University
Xiamen 361005 (China)
E-mail: dpzhan@xmu.edu.cn

[**] This work is supported by the National Science Foundation of China (NSFC, No. 20973142), the NSFC Innovation Group of Interfacial Electrochmistry (No. 21021002), National Project 985 of High Education, and New Faculty Starting Package of Xiamen University.

Supporting information for this article is available on the WWW under http://dx.doi.org/10.1002/anie.201103386.

increases with the increasing $Na_4Fe(CN)_6$ concentration. Third, the ratio of $Fe(CN)_6^{4-}$ over $Fe(CN)_6^{3-}$ can be adjusted through the applied potential of the substrate. The mixed-valent iron is crucial for electron transfer process in the solid-state solution.[6,7,14] Furthermore, the size of microcrystal can be controlled and optimized by proper choice of parameters, including the orifice size of the microcapillary and the hydrophobic properties of the substrate and the tip of the microcapillary, electrochemical modulation, and temperature.

The results of electron energy dispersive spectroscopy (EDS) indicate that the main component of the microcrystal is NaCl (Supporting Information, S2). To identify the iron hexacyanide components in the microcrystals, confocal Raman spectroscopy with a 633 nm laser excitation is adopted. Figure 2a shows the confocal Raman spectrum of a typical single microcrystal. By comparing with Raman spectra of pure Prussian blue, $Na_4Fe(CN)_6$, and $Na_3Fe(CN)_6$

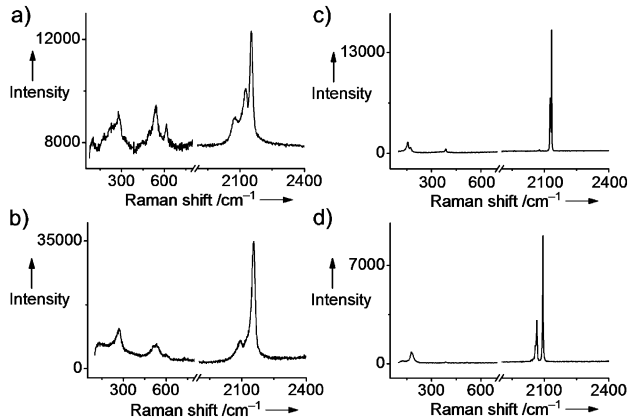

Figure 2. A confocal Raman spectra of microcrystals: a) synthesized through scanning microcapillary technique with a solution of 1.0×10^{-3} mol L^{-1} $Na_4Fe(CN)_6$ and 0.05 mol L^{-1} NaCl, b) Prussian blue, c) $Na_3Fe(CN)_6$, and d) $Na_4Fe(CN)_6$ crystals synthesized by a hydrothermal method.

crystals (Figure 2b–d), the bands in the region from 2000–2200 cm^{-1} of Figure 2a are assigned to the CN stretching, confirming that both $Fe(CN)_6^{3-}$ and $Fe(CN)_6^{4-}$ are present within the NaCl microcrystals. The Raman spectrum of Fe–C bands near 300 cm^{-1} and 530 cm^{-1} are characteristic of Prussian blue (PB), as reported previously.[15]

It was reported that the linear distance across the N≡C–Fe–C≡N group is about 9.12 Å for a ferricyanide complex and 9.32 Å for a ferrocyanide complex, the lattice parameter of PB is known to be 10.2 Å, whereas the distance across the Cl–Na–Cl group is 9.2 Å in NaCl crystals.[11,14] The size differences are within 15% in reference to the lattice size of NaCl crystal, which meets the requirement for the formation of a substitutional solid solution.[16] In other words, their size agreement would allow $NaCl_6^{5-}$ to be replaced by $Fe(CN)_6^{4-}$, $Fe(CN)_6^{3-}$, or PB units in NaCl crystals. In the cases of $Fe(CN)_6^{3-}$/$Fe(CN)_6^{4-}$ substitutions, Fe^{3+} or Fe^{2+} would occupy Na^+ site and six CN^- replace six neighboring Cl^- sites. Since Fe^{3+} and Fe^{2+} have a higher valence than Na^+, to achieve electrical neutrality, two positive cation vacancies are left for $Fe(CN)_6^{3-}$ as well as one for $Fe(CN)_6^{4-}$. Furthermore, the zeolitic nature of PB with channel diameters of 3.2 Å allows the diffusion of hydrated ions and low-molecular-weight molecules.[17,18] The crystal defects (vacancies and interstitials) make the counterion transfer possible in solid-state solution when the iron hexacyanides are oxidized or reduced, which is well elucidated in solid-state electrochemistry of PB and its analogues.[6,7,14,17–19]

Iron hexacyanides are well-known redox couples in aqueous solutions. Its behavior in the NaCl microcrystal is characterized by cyclic voltammetry, which is performed by fixing a microcapillary containing only 0.05 mol L^{-1} NaCl aqueous solution onto an as prepared NaCl microcrystal. Figure S3 (Supporting Information) shows typical voltammetric behavior of one single microcrystal. The voltammetric responses are stable and symmetric. The peak currents are in positive proportional to scan rates. The ratios of peak currents as well as charges associated with the anodic and cathodic processes are almost equal, and the peak-to-peak potential difference is less than 30 mV, which does not change with the scan rate. These features of the voltammogram show the characteristics of a reversible electrode reaction of surface immobilized redox species.[19]

The advantage of the solid-state redox microcrystal is its potential application to construct all solid-state electrochemical microdevices. To demonstrate the possibility of this kind of application, we fabricated the microcrystal in a micrometer-sized gap of gold ultramicrometer-scale electrode pairs on a microchip. A microcapillary with 4.6 μm-diameter orifice and containing an aqueous solution of 0.05 mol/L NaCl and 1.0×10^{-3} mol L^{-1} $Na_4Fe(CN)_6$, is positioned over the gap. The two gold microelectrodes, both as working electrodes, are subjected to a few potential scanning cycles from 0 to 0.5 V at a scan rate of 0.1 V s^{-1}. A microcrystal is thus fabricated, which is about 3 μm by 2 μm in size from top view and covers the gap between the two gold ultramicroelectrodes (Figure 3a). After drying in vacuum overnight, solid-state voltammetry is performed to examine the conductivity of the microcrystal and thus demonstrate its potential application in microdevices.

To do so, one of the gold microelectrodes is used as working electrode, while the other is used as both reference and counter electrodes. Well-defined voltammograms were obtained in a laboratory-made vacuum drier inside which freshly dried silica gel is placed on the bottom. The peak current is in positive proportional to the scan rate as shown in Figure 3b,c. It should be emphasized that the microcrystal is not exposed to any liquid, and the humidity inside the vacuum dry box is almost zero. The Faradic current must be due to the redox processes of iron hexacyanide substitutes in the lattice of solid NaCl microcrystals; that is, the solid-state redox solution. As discussed above, the electrons and the counterions hop along the solid-state crystal lattices oppositely to fulfill their transport.[6,7] Suppose the rate determining step is the hopping of electrons or counterions in a thin-layer of the solid-state solution, and analogous to the thin-layer behavior in liquid solution, the apparent concentration of iron hexacyanides can be estimated as 1.44×10^{-3} mol cm^{-3} from Equation (1):[20]

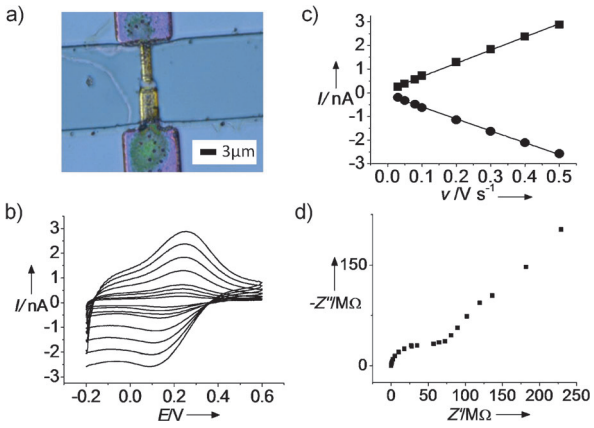

Figure 3. a) An optical image of the sample microdevice, where the microcrystal is fabricated through scanning microcapillary technique with an solution of 1.0×10^{-3} mol L^{-1} $Na_4Fe(CN)_6$ and 0.05 mol L^{-1} NaCl. The gap between the two gold ultramicroelectrodes is about 1.5 μm. b) All-solid-state cyclic voltammetric behavior of the redox microcrystal without exposure to any liquid environment; scan rates are 0.03, 0.05, 0.08, 0.1, 0.2, 0.3, 0.4, and 0.5 V s^{-1}. c) The linear relationship between the peak currents and the scanning rates. (d) Solid-state electrochemical impedance spectroscopy of the redox microcrystal. The impedance spectrum was recorded within a frequency range of 0.1 Hz–100 KHz at the potential of 0.2 V. The amplitude of the alternating voltage was 10 mV.

$$i_p = \frac{n^2F^2\nu VC}{4RT} \quad (1)$$

where, i_p is the peak current, n the electron transfer number, F Faraday constant, V the volume of the microcrystal, ν the scanning rate, C the apparent concentration of iron hexacyanides in the solid-state redox solution. If C_O is equal to C_R, the apparent electron transfer rate can be obtained as 1.6×10^{-4} cm s^{-1} through the electron transfer resistance value (58 MΩ) read-out from electrochemical impedance spectroscopy (EIS) as shown in Figure 3d.

In situ electrochemical modulated confocal Raman experiments were performed again to monitor the ratio of Fe^{III}/Fe^{II} complexes at the gold electrode/solid-state solution interface. Figure 4 shows the steady-state Raman spectra of the microcrystal polarized at different potentials. The Raman band at 2070 cm^{-1} and 2100 cm^{-1} are ascribed to the CN stretch in the Fe^{II} complex, and the band at 2125 cm^{-1} to those in the Fe^{III} complex. The intensity ratio of Fe^{III}/Fe^{II} are 0.14, 0.35, and 0.80 at 0.1, 0.3, and 0.5 V, respectively. The band of the CN stretch in the Fe^{III} complex becomes relatively stronger at the positive applied potential. The change of Raman intensity with the applied potential indicates its potential application into scintillators or electrocolorimeter.

In conclusion, we have presented a microfabrication technique based on scanning electrochemical microcapillary to synthesize microcrystals of solid-state redox solution, investigated the solid-state electrochemistry of the single microcrystals and their in-situ confocal Raman properties, and demonstrated its potential application as solid-state electrolyte valuable in the construction of electrochemical microdevices. Owing to the similar lattice structures, the transition metal cyanide complexes (such as Fe, Co, Ni, Rh, Ir, Pt, Pt) can also form solid-state redox solution in NaCl, KCl, or AgCl crystals.[11–14,21–28] As another example, the solid-state solution of $Co(CN)_6^{3-}$ in a NaCl microcrystal fabricated through this technique is shown in the Supporting Information, S4. These kinds of solid-state solution usually preserve some specific properties, such as electric conductivity and luminescent and electrochemical properties, which are not found in their aqueous solutions. The work presented herein is expected to promote practical application of electrochemical microsystem into all solid-state microdevices.

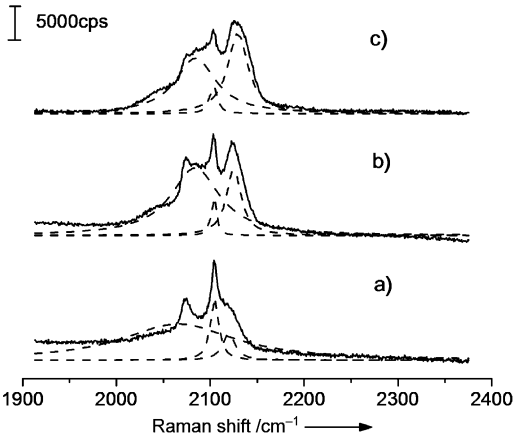

Figure 4. In-situ electrochemical modulated confocal Raman spectra of the same microcrystal constructed in the all solid-state microchip at different polarization potential: (a) 0.1 V, (b) 0.3 V, and (c) 0.5 V.

Experimental Section

All the chemicals used are analytical grade or better. All aqueous solutions are prepared with deionized water (18.2 MΩ, Milli-Q, Millipore Co.). The microcapillaries are prepared by the laser puller PS-2000 (Sutter Co.). The glass cover slides are coated with a thin film of gold by magnetron sputter deposition. The ITO glass cover slides are commercial available. Before each experiment, the slides are cleaned with acetone and deionized water several times and dried with pure nitrogen gas. All the electrochemical experiments are performed by the SECM workstation CHI920c (CHI Instrument Co.) combined with a video monitor. Electrochemical impedance spectroscopy (EIS) was carried out with a Parstat 2273 (Advanced Measurement Technolgy, Inc.). SEM, Raman, and AFM experiments were performed with HITACHI S-4800 Scanning Electron Microscope (Hitachi High-Technologies, Co.), Renishaw inVia Raman microscope (Renishaw Plc.), and Agilent 5500 AFM (Aglient Technologies, Co.), respectively. The more details of the experiment setup can be found in the Supporting Information, sections S5 and S6.

Received: May 17, 2011
Published online: July 26, 2011

Keywords: electrochemistry · microcapillaries · microfabrication · redox chemistry · solid-state solutions

[1] J. Korvink, O. Haber, *MEMS: A Practical Guide to Design, Analysis, and Applications*, William Andrew, New York, **2005**.
[2] H. Andersson, A. van den Berg, *Lab-on-chips for cellomics: micro and nanotechnologies for life science*, Kluwer, London, **2004**.

[3] B. J. Feringa, *Molecular Switches*, Wiley-VCH, Weinheim, **2001**.
[4] V. Balzani, A. Credi, M. Venturi, *Molecular Devices and Machines—A Journey into the Nano World*, Wiley-VCH, Weinheim, **2003**.
[5] W. Zhan, R. M. Crooks, *J. Am. Chem. Soc.* **2003**, *125*, 9934–9935.
[6] P. J. Kulesza, J. A. Cox, *Electroanalysis* **1998**, *10*, 73–80, and reference therein.
[7] P. J. Kulesza, Z. Galus, *Electrochim. Acta* **1997**, *42*, 867–872.
[8] C. G. Williams, M. E. Edwards, A. L. Colley, J. V. Macpherson, P. R. Unwin, *Anal. Chem.* **2009**, *81*, 2486–2495.
[9] For example: M. M. Lohrengel, A. Moehring, M. Pilaski, *Electrochim. Acta* **2001**, *47*, 137–141.
[10] J. F. Duncan, H. J. Percival, *Aust. J. Chem.* **1968**, *21*, 2175–2188.
[11] S. C. Jain, A. V. R. Warrier, H. K. Sehgal, *J. Phys. C* **1973**, *6*, 193–200.
[12] R. Kirmse, R. Bottcher, J. P. Willems, E. J. Reijerse, E. De Boer, *J. Chem. Soc. Faraday Trans.* **1991**, *87*, 3105–3111.
[13] P. V. Sushko, A. L. Shluger, R. C. Baetzold, C. R. A. Catlow, *J. Phys. Condens. Matter* **2000**, *12*, 8257–8266.
[14] For example: K. Itaya, I. Uchida, V. D. Neff, *Acc. Chem. Res.* **1986**, *19*, 162–168.
[15] H. G. M. Edwards, R. Wolstenholme, D. S. Wilkinson, C. Brooke, M. Pepper, *Anal. Bioanal. Chem.* **2007**, *387*, 2255–2262.
[16] P. J. Gellings, H. J. M. Bouwmeester, *The CRC Handbook of Solid State Electrochemistry*, CRC Press, New York, **1997**.
[17] A. A. Karyakin, *Electroanalysis* **2001**, *13*, 813–819.
[18] F. Ricci, G. Palleschi, *Biosens. Bioelectron.* **2005**, *21*, 389–407.
[19] F. Scholz, U. Schröder, R. Gulaboski, *Electrochemistry of Immobilized Particles and Droplets*, Springer, Heidelberg, **2005**.
[20] *Scanning Electrochemical Microscopy* (Eds.: A. J. Bard, M. V. Mirkin), Marcel Dekker, New York, **2001**.
[21] D. J. Carter, M. I. Ogden, A. L. Rohl, *Aust. J. Chem.* **2003**, *56*, 675–678.
[22] K. V. Reddy, T. R. Reddy, S. C. Jain, *J. Magn. Reson.* **1974**, *16*, 87–94.
[23] S. C. Jain, K. V. Reddy, T. R. Reddy, *J. Chem. Phys.* **1975**, *62*, 4366–4372.
[24] A. K. Visvanath, J. Vetuskey, W. D. Ellenson, M. B. Krogh-Jespersen, H. H. Patterson, *Inorg. Chem.* **1981**, *20*, 3493–3499.
[25] N. M. Pinhal, N. V. Vugman, *J. Phys. C* **1985**, *18*, 6273–6279.
[26] M. T. Bennebroek, J. Schmidt, R. S. Eachus, M. T. Olm, *J. Phys. Condens. Matter* **1997**, *9*, 3227–3240.
[27] R. C. Baetzold, *J. Phys. Chem. B* **1997**, *101*, 1130–1137.
[28] X. W. Li, R. J. Liu, A. C. Geng, S. P. Yang, G. S. Fu, *Chin. Phys.* **2005**, *14*, 404–408.

